A Dynamic Model for Aircraft Poststall Departure

M. A. Hreha*
and
F. H. Lutze†
Virginia Polytechnic Institute and State University, Blacksburg, Virginia

An aerodynamic model is developed for use with a numerical simulation of vehicle motion for the purpose of analyzing high-angle-of-attack behavior including poststall departure. The model consists of a nonlinear lifting line theory that includes unsteady wake effects due to a discrete, nonplanar vortex system. Each lifting surface is modeled with discrete vortex segments and their associated control points. The wing, horizontal, and vertical tail are treated in this manner. Application to a general-aviation-type vehicle indicates the effects of flight asymmetries and rate of stall penetration on poststall departure. In addition, forced oscillation wind tunnel tests in roll are simulated using this areodynamic model and are shown to agree quite well with actual tests for two different configurations.

Nomenclature

b = wing span
C_i = chord of ith panel
C_L = lift coefficient
$C_{\ell_{\dot\beta}}$ = $\partial C_\ell/\partial(\dot\beta b/2V)$
C_ℓ = rolling moment coefficient
C_{ℓ_p} = $\partial C_\ell/\partial(pb/2V)$
I_x, I_y, I_z = moment of inertia
p,q,r = angular rates about body x,y,z axes, respectively
$r^i_{j,k}$ = position vector from ith panel to wake vortex element j,k (j is the span number, k the wake number)
V = velocity
α = angel of attack
α_d = downwash angle of attack
α_{eff} = effective angle of attack
β = sideslip angle
$\Gamma_{j,k}$ = circulation strength (j is the span number, k the wake number)
$\Gamma_{j,l}$ = jth wing (tail) panel
δ_e = elevator deflection
θ = pitch angle
ϕ = roll angle
ψ = heading angle

Superscript
i = ith panel

Introduction

At a recent General Aviation Stall/Spin Workshop, it was said that aircraft "stall spin problems represent one of the last technical frontiers in the aviation field and have significant impact on (especially) the general aviation industry."[1] Although such a statement is rather dramatic, approximately 28% of all general aviation facilities are attributed to this realm of flight. Furthermore, this percentage has not changed over the last 15 years.[2] In order to improve these statistics, various segments of the general aviation industry have indicated the desirability of poststall analytic prediction techniques. An interesting quote from the opening remarks at NASA's 1980 Stall/Spin Workshop substantiated this need in that "the lack of validated analytical tools, together with many unsuccessful attempts to generalize results from one configuration test to another has added a considerable amount of testing to (Langley's) original planned program and lessened the number of stall/spin experts both at this Center and elsewhere."[3]

Although a considerable amount of experimental methods and flight test results were presented at the workshop, little work was presented in the area of analytical predictive techniques either completed or proposed. The work presented here represents an initial effort in the development of an analytical technique that can be used to predict vehicle behavior in the poststall region of flight.

Current analytical techniques include flight trajectory simulation on a digital computer, where vehicles are "flown" into high-angle-of-attack situations and the resulting gyrations obtained, and the application of small disturbance theory to various steady-state flight conditions, where steady-state spin motions are examined using linear eigenvalue, eigenvector analysis.[1,4-7] The sources of the procedures rest heavily on the validity of the aerodynamic data used. Typically, the data are obtained from computational methods or, more likely, from standard and specialized wind tunnel tests.[8-10] In most cases, the data are not extensive enough for the wide range of conditions likely to be encountered in stall-departure-spin studies and, further, most are typically not obtained under the dynamic conditions associated with aircraft stall and departure. Results obtained from these types of analysis have been shown under some circumstances to be sensitive not only to the data obtained but to the interpretation of that data as used in the simulation or analysis.[4] Finally, one can observe that because of the extensive data needed for complete simulation, either by computational methods or by wind tunnel tests, the use of these procedures early in the design of a vehicle would be difficult, especially if several configurations were to be studied.

From the discussion above it is clear that any valid analytical model for the stall-departure-spin aspect of flight must be capable of including the effects of nonlinear aerodynamics associated with the stall; unsteady aerodynamics associated with the possibly rapid vehicle motion; and the three-dimensional effects associated with this same motion. At the outset, it appears that a very sophisticated aerodynamic model is needed to satisfy all the above requirements. However, joining such a model with a numerical trajectory and vehicle motion simulation would be prohibitive in time and cost. Indeed, many current aerodynamic codes for just static considerations are prohibitive from this point of

Received Oct. 28, 1982; revision received July 10, 1983.

*Graduate Research Assistant; presently Senior Engineer, Technology, McDonnell Douglas Corporation, St. Louis, Mo.
†Professor, Aerospace and Ocean Engineering. Member AIAA.

view. Consequently, an aerodynamic package is required that retains the above properties but can be coupled with a vehicle motion simulation in an interactive manner. Furthermore, this aerodynamic package must easily accommodate changes in vehicle geometry if it is to be used early in the vehicle design process. The nonlinear lifting line procedure utilizing limited wind tunnel (or computational) data proposed below satisfies this requirement as well as those previously mentioned.

Nonlinear Lifting Line Procedure

The nonlinear lifting line procedure, which includes unsteady wake effects, has been developed by Levinsky and is outlined briefly here.[11] Its purpose is to obtain the time-dependent span load distributions of the various lifting surfaces and their associated contribution to the force and moment on the vehicle.

The lifting line assumption states that each spanwise panel of the surface acts like a two-dimensional airfoil at an effective angle of attack equal to the difference between the local pitch angle of attack and the downwash angle of attack induced by the trailing vortex system. For the panel i,

$$a^i_{\text{eff}}(t) = \alpha^i_p(t) - \alpha^i_d(t) \tag{1}$$

The theory assumes that the two-dimensional, steady-state, nonlinear relationship between the angle of attack and lift coefficient for a given airfoil section is imparted to the individual panel, and is known,

$$C^i_L(t) = C^i_L[\alpha^i_{\text{eff}}(t)] \tag{2}$$

Implicit in this assumption is the requirement that the chordwise pressure distribution achieves steady state in a shorter time scale than that associated with the wake and vehicle dynamics. The unsteady effects therefore enter through the local pitch angle of attack as a function of the vehicle motion, and through the induced angle of attack, which depends on the location and strength of the wake vortices, which, in turn, depend on past vehicle motion.

The induced angle of attack in Eq. (1) is obtained in the usual manner by summing the contributions to the downwash velocity at a control point due to the vortices in the trailing wake. The contribution of each wake vortex depends upon its location and strength. The detailed expressions are given by Levinsky[11] and, more generally, in Ref. 12. Functionally,

$$\alpha^i_d = \sum_{j=1}^{N} \sum_{k=1}^{M} f(r^i_{j,k}, \Gamma_{j,k}) \tag{3}$$

where j indicates the spanwise location of the vortex element, and k indicates the streamwise location of the element. The final equation needed is the Kutta-Joukoski law, which leads to

$$\Gamma_{i,1} = \tfrac{1}{2} V^i_N C_i C^i_L[\alpha^i_{\text{eff}}(t)] \tag{4}$$

Equations (1-4) can be formulated as a system of $2N$ algebraic equations in $2N$ unknown quantites, $\Gamma_{i,1}$ and α^i_{eff}, where $i = 1,2,\ldots,N$. Since Eq. (2) is a prescribed nonlinear lift curve, an iteration procedure must be employed to obtain a solution. Note that if a linear lift curve is used, the equations become linear in the unknown quantities and can be solved directly.

Dynamic Model

In order to develop a dynamic model for poststall departure, it is necessary that the nonlinear lifting line theory interact with the equations governing the vehicle motion. This interaction is the main contribution of this paper and allows the dynamic motion of stall and departure to be modeled.

The model is best described through the use of three coordinate systems: 1) body fixed, 2) panel fixed, and 3) inertial. The body fixed system is used to locate the lifting lines and control points for each panel. Three points characterize a given panel, the head and tail of the bound vortex segment, and the control point. These, in turn, are determined by inputting the basic geometry of the vehicle, such as wing position with respect to the center of gravity, dihedral, incidence angle, sweep angle, and number of panels per wing. Similar inputs are used for the horizontal tail and vertical fin (see Fig. 1). Once defined, the vortex and control point positions are fixed in the body fixed axes.

A local panel fixed system is used to apply the nonlinear lifting line theory. In particular the local angles of attack and downwash angles are determined using velocity components represented in this system. The local panel coordinate system can be determined from the three points defined in the body fixed system using vector algebra.[12] Once established, these

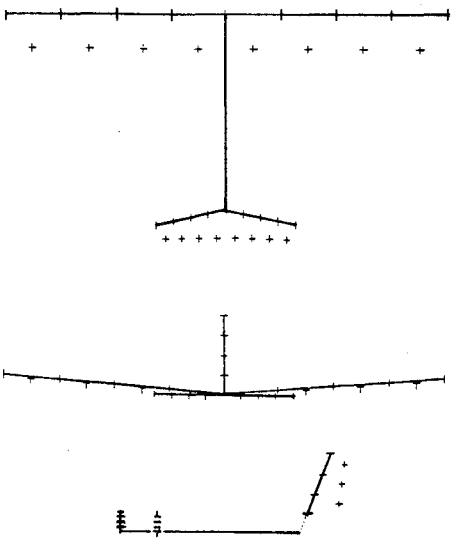

Fig. 1 Aircraft geometric model.

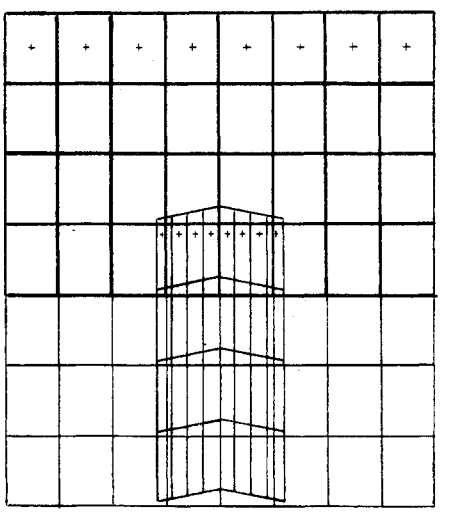

Fig. 2 Initial vortex geometry. Main wing downwash computed from eight spanwise by four streamwise parallelogram elements. Horizontal and vertical tail wash computed from eight spanwise by seven streamwise wing elements, eight spanwise by four streamwise tail plane elements, and three spanwise by four streamwise vertical tail elements.

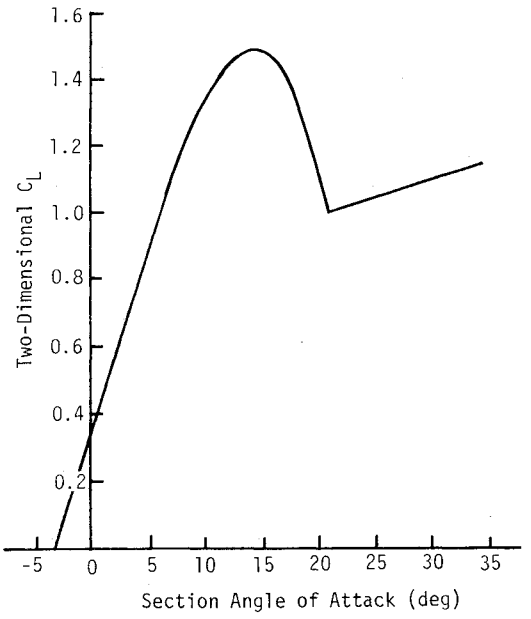

Fig. 3 Lift curve for basic 64_2-415 airfoil section.

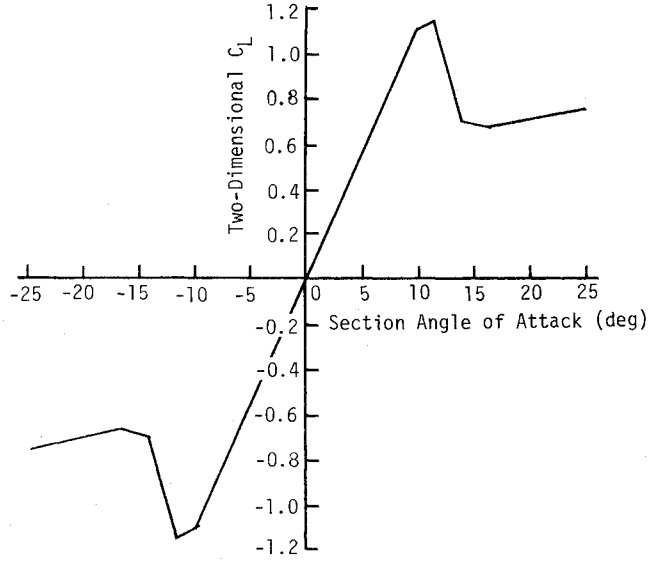

Fig. 4 Lift curve for 65_1-012 airfoil section.

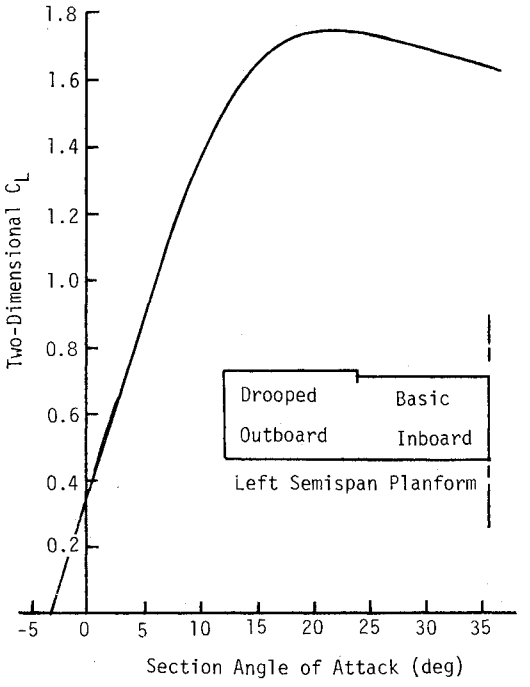

Fig. 5 Lift curve for 65_2-415 airfoil section with drooped leading edge.

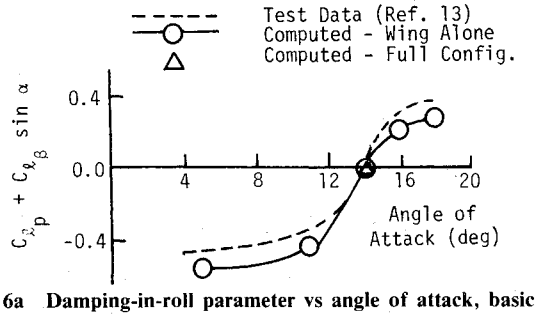

Fig. 6a Damping-in-roll parameter vs angle of attack, basic wing. Amplitude = ± 15 deg; frequency = 0.3 Hz.

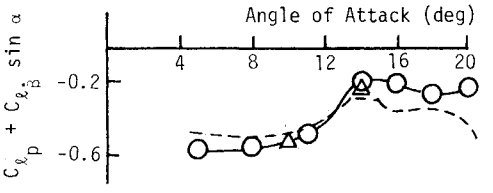

Fig. 6b Damping-in-roll parameter vs angle of attack, drooped outboard segmented wing. Amplitude = ± 15 deg; frequency = 0.3 Hz.

local systems are fixed in orientation and position with respect to the body fixed system.

Finally, an inertial coordinate system is needed to represent the trajectory of the aircraft, the attitude of the aircraft, and, finally, to locate the wake vortex positions with respect to the aircraft and, in particular, with respect to each panel. The orientation and position of the vehicle axes with respect to the inertial axes vary with time and is governed by the equations of motion. The wake vortex positions are assumed fixed with respect to the inertial system and are not allowed to drift.

A series of calculations were performed to determine the number of streamwise elements which must be retained for panel load calculations. In addition, the effects of the interaction between the tail and wing calculations were considered. It was found that tail effects on the wing were negligible and that no more than four (wing) chord lengths were needed downstream of a panel surface for accuracy within 1%. These considerations led to the panel vortex system shown in Fig. 2, which also is typical of an initial condition configuration with the wake for each lifting surface extending in a plane behind the surface.

A summary of the sequence of events which occurs during a simulation time step is as follows: At the beginning of each step, the vehicle linear and angular position and rates are known. The velocity and body angular rates allow the local angle of attack α_p^i to be determined. The location and strength of all the necessary wake vortices are known, and their orientation and position relative to the local panels can be determined. The nonlinear lifting line problem is now solved by guessing an induced downwash angle α_{d_i} and carrying out an iterative procedure as suggested by Levinsky.[11] Once converged, the local forces are computed and summed to obtain the overall force and moment used in the equations of motion to calculate the position and attitude for the beginning of the next time step. The vortices farthest downstream are dropped, and new wake vortices are added at the position and attitude of the panels from which they originate at the beginning of the time step. Details of convergence considerations are given in Ref. 12.

Aircraft Model

The above stall-departure dynamic model was coded to maintain complete flexibility as to aircraft geometry and initial flight conditions. The method was applied to the Grumman American AA-1 Yankee and the results presented here. The simple geometry, the large experimental data base, and NASA full-scale flight experience make this configuration a prime test candidate.

The airframe geometry and mass properties are listed in Table 1 (Ref. 13). The two-dimensional wing and tail lift curves for a NACA 64_2-415 and NACA 65_1-012, respectively, are shown in Figs. 3 and 4 (Ref. 14). Since two-dimensional data were not available past 20 deg, the three-dimensional data for the same wing section from Ref. 15 were modified.[12]

Flight tests demonstrating the usefulness of discontinuous outboard drooped leading edges for spin resistance led to the inclusion of this geometry in this investigation. The additional lift curve required for inclusion of a drooped leading edge section was obtained by modifying the three-dimensional data from Ref. 16, with results shown in Fig. 5 (Ref. 12). Since lifting line theory does not predict drag very well, the axial force coefficients obtained from static wind tunnel tests were used.[12,13] It is suspected that the departure motions are not strongly influenced by the drag model used.

Results and Discussion

Initially, the wing-alone configuration was examined in steady state and in pitch oscillation motions. For the steady-state solutions below stall, all panels were unstalled and the lift was distributed symmetrically about the centerline. For steady-state solutions above stall, the spanwise lift distribution was not unique. In particular, not all the panels would stall leading to regions of stall or stall cells on the wing. These cells are consistent with experimental results observed in Ref. 17.

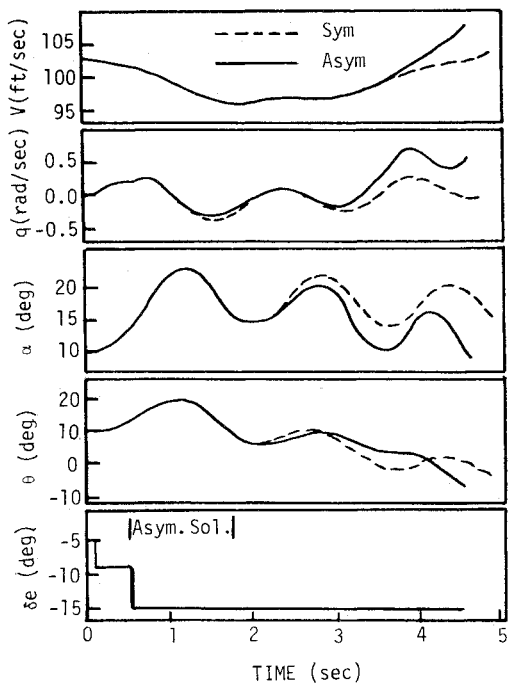

Fig. 7a Symmetric stall penetration—basic wing, longitudinal parameters.

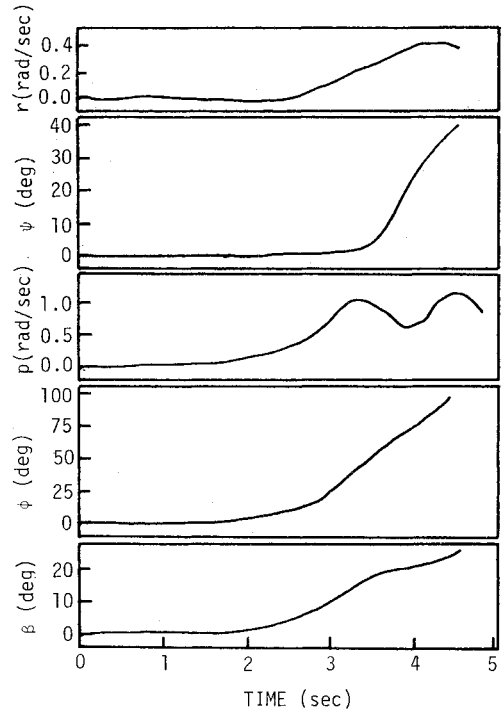

Fig. 7b Symmetric stall penetration—basic wing, lateral parameters, asymmetric induced angle-of-attack solution.

Table 1 Aircraft mass and geometry characteristics

Aircraft	Weight, lb	I_x slug-ft^2	I_y	I_z
	1543	609	745	1284

	Span, ft	Dihedral, deg	Incidence	Sweep
Wing	24.46	5.0	3.5	0.0
Tail	7.46	0.0	Variable	11.93
Fin	3.375	90.0	0.0	20.56

Panel chord lengths, ft

No.	1	2	3	4	5	6	7	8
Wing	4.0	4.0	4.0	4.0	4.0	4.0	4.0	4.0
Tail	1.848	2.203	2.559	2.915	2.915	2.559	2.203	1.848
Fin	3.040	2.527	2.015	...	...	...	...	...

Location of 25% $\bar{C}$, ft

	X	Y	Z (+ down)
Wing	0.04	0	0
Tail	−11.0	0	0
Fin (bottom panel)	−10.395	0	−1.053

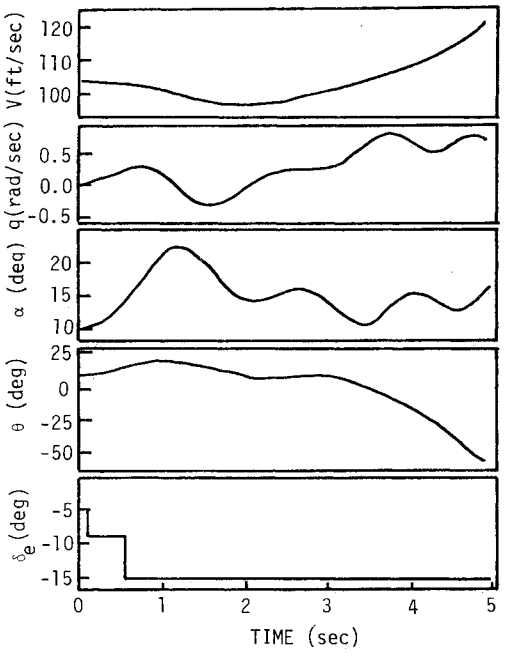

Fig. 8a Asymmetric stall penetration—basic wing's longitudinal parameters, initial sideslip angle = −5 deg.

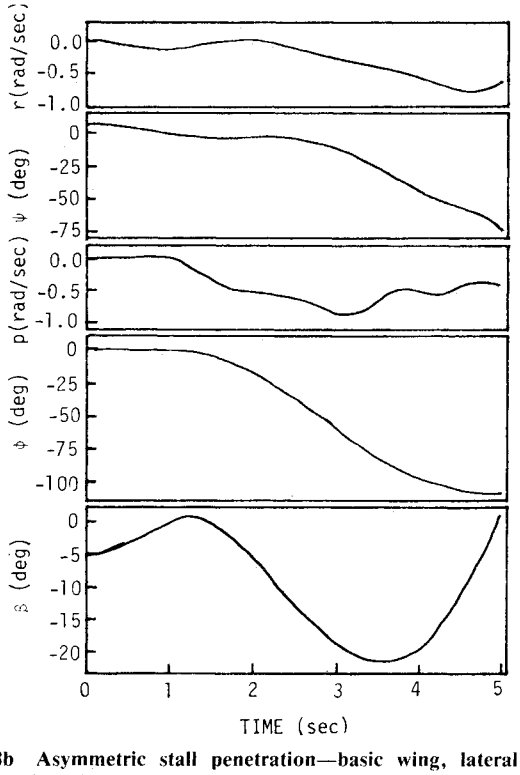

Fig. 8b Asymmetric stall penetration—basic wing, lateral parameters, initial sideslip angle = −5 deg.

Additional discussion regarding the observation of stall development in experimental tests is given in Refs. 18 and 19. In addition, asymmetric solutions are obtainable for angle of attack above stall. These are obtained by initiating asymmetric guesses in the iterative procedure described previously. These solutions were expected, as indicated in Ref. 20. As a result of these asymmetric solutions, it is possible to obtain rolling moments in symmetrical flight conditions, a possible, important factor in initiating a departure motion.

The pitch oscillation simulations in the neighborhood of the stall angle of attack showed the unsteady aerodynamic effects through the development of hysteresis in the lift-angle of attack curves. These results were demonstrated in Ref. 11 and are shown to be dependent on the procedure used to select an initial guess for the induced angle of attack distribution in the lifting line solutions. Here, and throughout the remainder of the results presented, the previous solution was used as an initial guess for unstalled panels, while an angle well past the stall was used for an initial guess for panels that were stalled in the previous time step. Such a scheme tends to accentuate any hysteresis effects.

Forced-Roll Oscillation

Following the static and pitch oscillation solutions just discussed, the dynamic model was used to simulate forced-roll oscillation wind tunnel tests. This is accomplished by specifying a fixed forward velocity and a fixed pitch angle. Furthermore, a sinusoidal motion in roll about the X vehicle axis is specified. The resulting roll moment measured out-of-phase with the rolling motion can be used to determine the dynamic stability parameter $C_{\ell_p} + C_{\ell_{\dot{\beta}}} \sin \alpha$ (Ref. 21). Such a simulation was run for the basic wing, for the complete configuration, and for the wing with a drooped leading edge on the outboard panels. This change in configuration is obtained by simply entering the two-dimensional lift curve slope for the drooped leading edge into the data for the two outboard panels of each wing. The results are presented in Fig. 6, where they are compared with actual results taken from wind tunnel tests for the complete aircraft.[13]

It should be noted that there is no fuselage modeling in the current dynamic model and that the drooped leading edge of the actual aircraft included the outboard 38% of the wing as opposed to the 50% in the dynamic model. In spite of these differences, Fig. 6 indicates that the dynamic model predicts the major characteristics of the angle of attack effect on the damping-in-roll parameter $C_{\ell_p} + C_{\ell_{\dot{\beta}}} \sin \alpha$. Furthermore, the time histories and spanwise distribution of the lift throughout each oscillation cycle can be studied in detail, if desired, and the mechanism associated with the sudden change in the damping-in-roll parameter determined.[12] The success of the forced-roll oscillation calculations also lends credence to the utility of the model in simulating poststall flight departures.

Stall-Departure Numerical Flight Simulations

The main objective of this dynamic model is to simulate poststall-departure flight motions. The pitch control of the aircraft is obtained by adjusting the incidence angle of the horizontal tail. All trajectories are flown from an initial condition of 10-deg angle of attack. The horizontal tail is given a step increment to −9 deg until the aircraft penetrates the stall, after which a full deflection of −15 deg is applied. The initial velocity is at 103 ft/s at an altitude of 3000 ft.

The trajectories presented represent investigations of three poststall phenomena: 1) the existence of multiple lifting line solutions, 2) the effect of flight asymmetries during stall penetration, and 3) the effect of configuration modifications on departure.

The dotted lines in Fig. 7a represent the time histories of the longitudinal variables of the Yankee Aircraft as it penetrates the stall. There are no initial flight asymmetries, and the induced angle of attack distribution required at the beginning of each iteration procedure is taken to be the last converged solution. The lateral variables are all flat zeros throughout and not presented. An identical trajectory is described by the solid lines in Fig. 7 except that, beginning with stall penetration, an asymmetric induced angle distribution was input as an initial guess in the lifting line solution iteration at every time step for an arbitrary 30 intervals. Both longitudinal and lateral variables are shown for this wing drop departure motion. The influence of asymmetric flight conditions is examined in Fig. 8, where an initial sideslip of −5 deg is prescribed (but no asymmetric initial guess). Again, both longitudinal and lateral variables are presented. Finally, Fig.

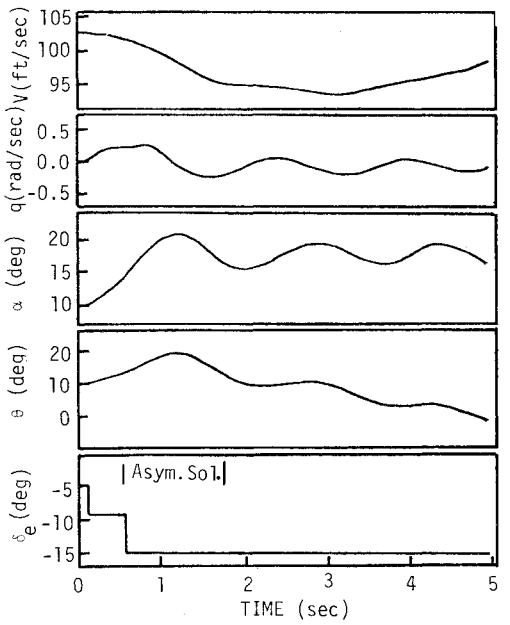

Fig. 9a Symmetric stall penetration—outboard drooped leading-edge, longitudinal parameters, asymmetric induced angle-of-attack solution.

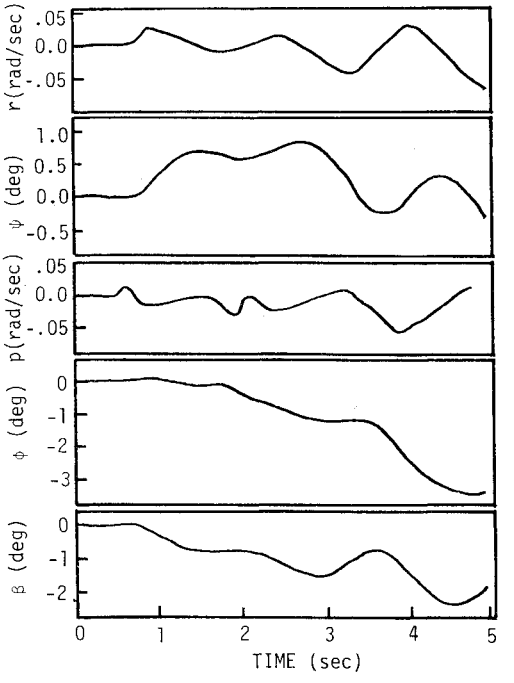

Fig. 9b Symmetric stall penetration—outboard drooped leading edge, lateral parameters, asymmetric induced angle-of-attack solution.

9 repeats the scenario of Fig. 7 for an aircraft with drooped leading edges on the outboard panels.

The symmetric motion shown in Fig. 7 represents a short period oscillation of about 1.4 s. As the aircraft pitches through stall, the wing vortex segments stall symmetrically, causing a loss of lift and a nose-down pitching moment due to the unstalled tail. As the nose drops, the wing unstalls, causing a nose-up moment and forcing another stall penetration. This "staggering motion of an aircraft" is called "mush."[2] This motion has not been recorded in flight tests of the Yankee configuration modeled here, suggesting that another poststall flight solution exists. It is suggested that slow stall penetration may lead precisely to this mushing solution.

In Fig. 7, the same entry conditions were initiated, but the lifting line procedure was encouraged to find an asymmetric solution by starting with an asymmetric iterate. Subsequently, the previous solution was assumed as the starting iterate. The resulting motion is a sharp wing drop to the right, with the aircraft rolling through 90 deg in 2.4 s. This poststall rolloff is characteristic of the full-scale Yankee.[13] Further study of the spanwise lift distribution with time indicates that an asymmetric lift distribution is obtained well before maximum angle of attack is obtained. However, the duration of the associated rolling moment is too short to produce rolloff. As the aircraft pitches into deep stall (all wing elements stalled), the asymmetric distribution virtually vanishes. The large sustained rolling moments occur in the asymmetric *unstalling* of the wing panels, particularly the most outboard ones. A similar simulation, where the aircraft was trimmed such that the wing was partially stalled, led to an asymmetric solution and an associated gentle rolloff. Hence the proper inclusion of the pitch dynamics associated with the stall penetration is important for the prediction of the departure characteristics.

In Fig. 8, the asymmetric flight condition is held into the stall with no asymmetric solution forced. The asymmetric flight condition was enough to trigger the asymmetric lifting line solutions leading to the wing drop departure mode. It is speculated here that fuselage effects should be included to get the true asymmetric flow pattern due to asymmetric flight. In any case, it may be concluded that small flight asymmetries prior to stall can induce abrupt departures, an effect noted in Yankee flight tests.

Finally the use of passive aerodynamic methods for preventing stall is illustrated in Fig. 9. The asymmetric solution is introduced as in Fig. 7, but the outboard panels never stall, precluding any large rolling moments causing wing drop. These results are clearly observed in the full-scale flight tests.[13]

Conclusion

The dynamic model presented has many of the necessary ingredients for simulating stall-departure motion of an aircraft. In particular, an interaction involving both aerodynamics and vehicle dynamics is included along with nonlinear and unsteady aerodynamic effects. The model is extremely flexible and is easily adapted to different configurations. Further, the model appears to predict the major departure motions observed in an actual flight test. In addition, simulation of a dynamic roll-oscillation wind tunnel test yields good results through all angles of attack below and above stall.

The model presented is considered an initial effort and clearly needs considerable "fine tuning." The results to date regarding the simulated forced oscillation wind tunnel tests and the departure motions are quite encouraging. Since the fuselage as well as the lateral-directional control surface deflections are not included in the model, it is a little premature to attempt direct comparisons with flight data. However, the trends, magnitudes, and time histories of the simulated results compare favorably with the flight test.

References

[1] *Summary of 1980 General Aviation Stall/Spin Workshop,* NASA-Langley Research Center, Hampton, Va., Sept. 1980.

[2] Silver, B. W., "Statistical Analysis of General Aviation Stall Spin Accidents," SAE Paper 760480, April, 1976.

[3] Stickle, J. W., "Preface," NASA-Langley Research Center General Aviation Stall/Spin Workshop, Hampton, Va., Sept. 1980.

[4] Hreha, M. A. and Lutze, F. H., "Linear Analysis of Poststall Gyrations," *Journal of Aircraft,* Vol. 17, Oct. 1980, pp. 727-733.

[5] McCain, C. E., "Utilization of Aerodynamic Coefficients Generated by Pure Yawing and Rolling Flow in the Determination of Aircraft Equilibrium Spin Properties," M. S. Thesis, Virginia Polytechnic Institute and State University, Blacksburg, Va., June 1978.

[6]Hreha, M. A., "Linear Analysis of Incipient Spin Dynamics," M. S. Thesis, Virginia Polytechnic Institute and State University, Blacksburg, Va., June 1979.

[7]Anglin, E. L., "Aerodynamic Characteristics of Fighter Configurations During Spin Entries and Developed Spins," *Journal of Aircraft*, Vol. 15, Nov. 1978, pp. 769-776.

[8]Bihrle, W., "Rotary-Balance Force Tests and Analysis of Equilibrium Spin Modes," NASA-Langley Research Center General Aviation Stall/Spin Workshop, Hampton, Va., Sept. 1980.

[9]Bihrle, W., Hultberg, R. S., and Mulcay, W.; "Rotary Balance Data for a Typical Single Engine Low-Wing General Aviation Design for an Angle-of-Attack Range of 30 to 90 deg," NASA CR-2972, July 1978.

[10]Bihrle, W., "Static Aerodynamic Characteristics of a Typical Single-Engine Low-Wing General Aviation Design for Angle-of-Attack Range of −8 to 90 deg," NASA CR-2971, July, 1978.

[11]Levinsky, E. S., "Theory of Wing Span Loading Instabilities Near Stall," *Prediction of Aerodynamic Loading*, AGARD-CP-204, 1976.

[12]Hreha, M. A., "A Dynamic Model for Aircraft Poststall Departure," Ph.D. Dissertation, Virginia Polytechnic Institute and State University, Blacksburg, Va., May, 1982.

[13]"Exploratory Study of the Effects of Wing-Leading-Edge Modifications on the Stall/Spin Behavior of a Light General Aviation Airplane," NASA TP-1589, Dec. 1979.

[14]Abbott, I. H., and Von Doenhoff, A. E., *Theory of Wing Sections*, Dover Publications, New York, 1959.

[15]Kroeger, R. A. and Feistel, T. W., "Reduction of Stall-Spin Entry Tendencies Through Wing Aerodynamic Design," SAE Paper 76-0481, April, 1976.

[16]Johnson, J. L., Newsom, W. A., and Satran, D. R., "Full-Scale Wind-Tunnel Investigation of the Effects of Wing Leading-Edge Modifications on the High Angle-of-Attack Aerodynamic Characteristics of a Low-Wing General Aviation Airplane," AIAA Paper 80-1844, Aug. 1980.

[17]Winkelmann, A. E., "Flourescent Oil Flow Studies of Stall Development of Wings," NASA-Langley Research Center General Aviation Stall/Spin Workshop, Hampton, Va., Sept. 1980.

[18]Meznarsie, V. F. and Gross, L. W., "Experimental Investigation of a Wing with Controlled Midspan Flow Separation," *Journal of Aircraft*, Vol. 19, June 1982, pp. 435-441.

[19]Gregory, N., Quincey, V. G., O'Reilly, C. L., and Hall, D. J., "Progress Report on Observations of Three-Dimensional Flow Patterns Obtained During Stall Development on Aerofoils and on the Problem of Measuring Two-Dimensional Characteristics," British ARP CP-1146, 1971.

[20]Sears, W. R., "Some Recent Developments in Airfoil Theory," *Journal of Aerospace Sciences*, Vol. 23, May 1956, pp. 490-499.

[21]Chambers, J. R. and Grafton, S. B., "Static and Dynamic Longitudinal Stability Derivaties of a Powered 1/9 Scale Model of a Tilting-Wing V/STOL Transport," NASA TN D-3591, May 1966.